

# Spatiotemporal changes of eutrophication and heavy metal pollution in the inflow river system of Baiyangdian after the establishment of Xiongan New Area

Yibing Wang<sup>Equal first author, 1, 2</sup>, Yang Wang<sup>Equal first author, 3</sup>, Wenjie Zhang<sup>1</sup>, Xu Yao<sup>1</sup>, Bo Wang<sup>1</sup>, Zheng Wang<sup>Corresp. 1, 2</sup>

<sup>1</sup> College of Forestry, Hebei Agricultural University, Baoding, China

<sup>2</sup> Hebei Urban Forest Health Technology Innovation Center, Baoding, China

<sup>3</sup> College of Land and Resources, Hebei Agricultural University, Baoding, China

Corresponding Author: Zheng Wang

Email address: wzhwangzheng@126.com

Pollution in inflow rivers seriously endangers the water environment in downstream lakes. In this study, an inflow river system of Baiyangdian–Fuhe river system (FRS) was investigated to display timely pollution patterns of eutrophication and heavy metals after the establishment of Xiongan New Area, aiming to reveal the weak parts in current pollution treatments and guide the further water quality management. The results showed that the pollution of eutrophication was worse than the heavy metals in FRS, with serious eutrophic parameters of ammonia nitrogen ( $\text{NH}_4^+\text{-N}$ ) and chemical oxygen demand (COD). There were greatly spatiotemporal variations of the pollution in FRS. 1) Concentrations of  $\text{NH}_4^+\text{-N}$  and total phosphorus were all higher in summer and autumn, whereas, COD contents were higher in spring; the water quality index (*WQI*) of eutrophication linearly increased along FRS in summer and autumn, with pollution hotspots around the estuary area. 2) The pollution levels of plumbum exceeded cadmium (Cd) and chromium (Cr) but without strongly spatiotemporal changes, however Cd and Cr in the town area and Cd in spring showed higher concentrations; the *WQI* of heavy metals showed single peak curves along FRS, with significantly higher values around the town area. Additionally, the four potential pollution sources: domestic sewage, traffic pollution, agricultural wastewater and polluted sediments were identified based on the pollution patterns and pollutant associations. These findings demonstrated current treatments failed to eliminate the pollution in some hotspots and periods, and the in-depth understanding of the pollution spatiotemporal patterns in this study, especially the pollution hotspots, serious periods and potential sources, are crucial to furtherly develop spatiotemporally flexible pollution treatment strategies.

1 Spatiotemporal changes of eutrophication and heavy metal  
2 pollution in the inflow river system of Baiyangdian after the  
3 establishment of Xiongan New Area

4

5 Yibing Wang<sup>1,2†</sup>, Yang Wang<sup>3†</sup>, Wenjie Zhang<sup>1</sup>, Xu Yao<sup>1</sup>, Bo Wang<sup>1</sup>, Zheng Wang<sup>1,2\*</sup>

6

7 <sup>1</sup> College of Forestry, Hebei Agricultural University, Baoding, Hebei Province, China

8 <sup>2</sup> Hebei Urban Forest Health Technology Innovation Center, Baoding, Hebei Province, China

9 <sup>3</sup> College of Land and Resources, Hebei Agricultural University, Baoding, Hebei Province,

10 China

11 † Yibing Wang and Yang Wang contributed equally to this work.

12

13 \*Corresponding Author:

14 Zheng Wang<sup>1,2</sup>

15 Lekai street No. 2596, Baoding, Hebei Province, 071000, China

16 Email address: [wzhwangzheng@126.com](mailto:wzhwangzheng@126.com)

17

## 18 **Abstract**

19 Pollution in inflow rivers seriously endangers the water environment in downstream lakes. In this  
20 study, an inflow river system of Baiyangdian–Fuhe river system (FRS) was investigated to  
21 display timely pollution patterns of eutrophication and heavy metals after the establishment of  
22 Xiongan New Area, aiming to reveal the weak parts in current pollution treatments and guide the  
23 further water quality management. The results showed that the pollution of eutrophication was  
24 worse than the heavy metals in FRS, with serious eutrophic parameters of ammonia nitrogen  
25 ( $\text{NH}_4^+\text{-N}$ ) and chemical oxygen demand (COD). There were greatly spatiotemporal variations of  
26 the pollution in FRS. 1) Concentrations of  $\text{NH}_4^+\text{-N}$  and total phosphorus were all higher in  
27 summer and autumn, whereas, COD contents were higher in spring; the water quality index  
28 (*WQI*) of eutrophication linearly increased along FRS in summer and autumn, with pollution  
29 hotspots around the estuary area. 2) The pollution levels of plumbum exceeded cadmium (Cd)  
30 and chromium (Cr) but without strongly spatiotemporal changes, however Cd and Cr in the town  
31 area and Cd in spring showed higher concentrations; the *WQI* of heavy metals showed single  
32 peak curves along FRS, with significantly higher values around the town area. Additionally, the  
33 four potential pollution sources: domestic sewage, traffic pollution, agricultural wastewater and  
34 polluted sediments were identified based on the pollution patterns and pollutant associations.  
35 These findings demonstrated current treatments failed to eliminate the pollution in some hotspots  
36 and periods, and the in-depth understanding of the pollution spatiotemporal patterns in this study,  
37 especially the pollution hotspots, serious periods and potential sources, are crucial to furtherly  
38 develop spatiotemporally flexible pollution treatment strategies.

39

## 40 **Introduction**

41 Water quality of inland waters is increasingly disconcerting for a long period due to the  
42 hazardous impacts of water deterioration in the world (Huang et al., 2019; Tong et al., 2017;  
43 Wang et al., 2021a). The water quality of inland waters is determined by numerous factors such  
44 as climate, hydrologic conditions, and anthropogenic activities (Sinha et al., 2017; Wang et al.,  
45 2021a; Zhuang et al., 2019). Generally, land use intensification and urbanization with increased  
46 population density have been considered as the most important driving factors for the declining  
47 water quality in inland waters (Huang et al., 2019; Tong et al., 2017; Zhou et al., 2017), which  
48 resulted in the increased wastewater discharge from households, agriculture and industry (Meng  
49 et al., 2021; Tong et al., 2017; Zhou et al., 2017). In China, inland waters are generally  
50 surrounded by densely populated areas, and the severe contamination has occurred in these  
51 inland waters, such as Taihu, Dianchi and Poyang lakes (Lv et al., 2020; Wang et al., 2021a; Wu  
52 et al., 2017), as well as Baiyangdian (Li et al., 2021a; Meng et al., 2021; Zhang et al., 2018). The  
53 water quality of inland waters has been extensively studied with special emphasis on topics, such  
54 as eutrophication (Sinha et al., 2017; Tong et al., 2017) and nutrient loading (Ni et al., 2016; Tao  
55 et al., 2020; Zhu et al., 2019). Eutrophication due to phosphorus and nitrogen pollution has posed  
56 a risk to the health and stability of the aquatic ecosystem, and ammonia nitrogen ( $\text{NH}_4^+\text{-N}$ ), total  
57 phosphorus (TP) and chemical oxygen demand (COD) are three important parameters of  
58 eutrophication in inland waters (Li et al., 2021b; Meng et al., 2021; Ni et al., 2016; Tong et al.,  
59 2017; Zhao et al., 2020). Water pollution caused by heavy metals also has caused widespread  
60 concern due to their health threat to aquatic biota and humans (Rajeshkumar and Li, 2018; Zhang  
61 et al., 2017; Zhang et al., 2019). At present, heavy metal pollution displayed an increasing trend  
62 in many lakes and reservoirs in China (Huang et al., 2019), and a large number of heavy metals

63 were still released from historical polluted sediments, causing a high risk of contamination to the  
64 aquatic ecosystem (Ke et al., 2017; Vu et al., 2017; Zhang et al., 2018).

65       Pollution in inflow rivers seriously endangers the water environment in downstream lakes.  
66 Comprehensive measures have been made regarding pollution reduction in inland waters in last  
67 decades (Chen et al., 2021a; Wang et al., 2021b; Zhou et al., 2017), however, the serious  
68 pollutions were still frequently observable due to the measures not taking serious consideration  
69 of the water pollution in inflow rivers (Gao et al., 2021; Lv et al., 2020; Wang et al., 2021a). The  
70 inflow rivers and the stream networks could collect domestic, agricultural and industrial  
71 wastewater from densely populated areas in the whole watershed, which have become the main  
72 reason for the water deteriorating in the downstream waters (Aubriot et al., 2020, Gao et al.,  
73 2021; Lv et al., 2020; Wang et al., 2021a; Wang et al., 2021b). In addition, the dominant  
74 contributor to the pollutants were presently changed from point source pollution (e.g., local  
75 industries) to the diffuse source pollution and internal pollution loading, which had greatly  
76 spatiotemporal variations along the inflow river systems (Huang et al., 2018; Wang et al., 2017;  
77 Xia et al., 2018; Zha et al., 2018; Zhu et al., 2019). A single pollution control method could not  
78 deal with the spatiotemporally varied pollution (Huang et al., 2018; He et al., 2020). Thus, water  
79 quality management strategies could hardly be successful unless the spatiotemporal variation of  
80 water pollution are taken into serious consideration, and spatiotemporal flexible measures should  
81 be furtherly made along the inflow rivers for the greater improvement of water quality (Aubriot  
82 et al., 2020; Gao et al., 2021; He et al., 2020; Wang et al., 2021a).

83       Water quality of inland waters in the North China Plain was found to be the poorest in  
84 China due to the high coverage of developed land (cities and cropland) and population density  
85 (Zhou et al., 2017). In addition, the relatively increased evaporation in this region created more

86 protracted periods of drought in spring and early summer, which prolonged the water retention  
87 time and amplifying the deterioration of water quality in inland waters (Piao et al., 2010; Sinha et  
88 al., 2017). Baiyangdian is the largest lake in North China Plain, playing an irreplaceable role in  
89 maintaining the environmental health in this region (Cheng et al., 2018; Guo et al., 2015; Yi et  
90 al., 2020; Zhao et al., 2021). However, with the rapid development of industry and agriculture,  
91 tons of pollutants were discharged into the water of inflow river systems and Baiyangdian since  
92 1980s, which not only severely contaminated of the water body but also the sediments and  
93 aquatic biota (Guo et al., 2015; Meng et al., 2021; Tao et al., 2020). The Xiongan New Area  
94 started to be built around Baiyangdian in 2017, which aimed to establish an advanced new area  
95 for the coordinated development of ecology and economy in China (Xia and Zhang, 2017). Since  
96 then, the water quality of Baiyangdian has been greatly concerned (Cheng et al., 2018; Meng et  
97 al., 2021; Zhao et al., 2021). The Chinese central and local governments have made substantial  
98 investments to environmental remediation in order to improve the water quality in Baiyangdian  
99 watershed to guarantee the healthy development of Xiongan New Area (Chen et al., 2021a; Xia  
100 and Zhang, 2017; Zhao et al., 2021). Presently, point source pollution has been basically  
101 controlled (Chen et al., 2021a; Li et al., 2021a). However, the water pollution in Baiyangdian  
102 was still in a high level, especially the severely eutrophic parameters of  $\text{NH}_4^+\text{-N}$ , TP and COD,  
103 as well as the serious heavy metal pollution of Plumbum (Pb), cadmium (Cd) and chromium (Cr)  
104 in the water and sediments (Li et al., 2021b; Gao et al., 2019; Meng et al., 2021; Zhao et al.,  
105 2021). The diffuse source pollution in this watershed became a main problem, such as  
106 agricultural sewage, domestic garbage and sediment release (Li et al., 2017; Li et al., 2021a; Tao  
107 et al., 2020; Zhu et al., 2019), which were carried by the inflow rivers from the whole watershed  
108 to contaminate the water environment in Baiyangdian and Xiongan New Area (Meng et al.,

109 2021; Tao et al., 2020; Zhao et al., 2020). Thus, eliminating the diffuse source pollution of the  
110 inflow rivers is critically important for the improvement of the water quality in Baiyangdian (Li  
111 et al., 2021a; Zhao et al., 2020; Zhao et al., 2021), and a flexible set of measures for water  
112 pollution control should be adopted considering the spatiotemporal differences of the diffuse  
113 source pollution (He et al., 2020; Huang et al., 2018; Tong et al., 2017). Surprisingly, our  
114 literature review has found that the spatiotemporal distributions and variability of water pollution  
115 in the inflow rivers of Baiyangdian has not been explored since the establishment of Xiongan  
116 New Area, particularly, we lack the timely understanding about the pollution hotspots, serious  
117 periods and potential sources in a whole inflow river system to distinguish the weak parts in  
118 current pollution treatments.

119 In this study, a typical inflow river system of Baiyangdian–Fuhe river system (FRS) was  
120 selected, which is one of the main water sources of Baiyangdian and passes through a big city, as  
121 well as many towns and villages (Cheng et al., 2018; Guo et al., 2015). Thus, FRS received  
122 strong impact of anthropogenic activities and was considered as one of the most seriously  
123 polluted inflow rivers of Baiyangdian (Li et al., 2017; Liang et al., 2017). To better guide the  
124 pollution control strategies, we measured the water eutrophication ( $\text{NH}_4^+\text{-N}$ , TP and COD) and  
125 heavy metal pollution (Pb, Cd and Cr) of the FRS from the headstream to the estuary in three  
126 seasons to investigate the spatiotemporal pollution pattern, identify the pollution hotspots and  
127 periods, and make a timely assessment of the water quality after the establishment of Xiongan  
128 New Area. We aimed to reveal the weak parts in current pollution treatments, and provide  
129 scientific basis to make spatiotemporally flexible measures for water quality improvement in  
130 Baiyangdian watershed. This study could be a reference for the water pollution treatment and  
131 ecological restoration in other inland waters.

132

## 133 **Materials & Methods**

### 134 **Study Area**

135 Baiyangdian Lake, located in north latitude  $38^{\circ}43'$ – $39^{\circ}02'$ , east longitude  $115^{\circ}38'$ –  
136  $116^{\circ}07'$ , lies in the semiarid warm temperate continental monsoon climate zone with four distinct  
137 seasons. The average annual precipitation is 539.7 mm, and 80% of the precipitation is  
138 concentrated in June to August (Cheng et al., 2018; Yi et al., 2020). Baiyangdian stays in the  
139 middle reaches of Daqing River System in Haihe River Basin, undertaking the floodwater  
140 storage of nine rivers, with a total area of 366 km<sup>2</sup> and an average annual water storage capacity  
141 of 1.32 billion m<sup>3</sup> (Xia and Zhang, 2017; Zhao et al., 2021). Baiyangdian is the biggest natural  
142 wetland in the North China Plain and locates in the south part of the Xiongan New Area, which  
143 has direct and significant influences on the ecological health of this region (Cheng et al., 2018;  
144 Xia and Zhang, 2017; Zhang et al., 2018). However, due to the influence of anthropogenic  
145 activities in recent decades, a large number of point and diffuse source pollutants flowed into  
146 Baiyangdian lake through the upstream river systems, endangering the water ecological  
147 environment and causing serious eutrophication and heavy metal pollution (Guo et al., 2015; Li  
148 et al., 2021a; Meng et al., 2021; Zhao et al., 2020).

### 149 **Sample collection**

150 A typical inflow river system of Baiyangdian–Fuhe river system (FRS) was selected to  
151 study the spatiotemporal pollution patterns and assess the water quality. Sampling was carried  
152 out sequentially along FRS from the headstream to the estuary area, taking into account of the  
153 topographic distribution, flow path distance and surrounding land uses, and a total of fourteen  
154 sampling sites were set up (Fig. 1). The source of FRS is located in the Mountain area in the west

155 of Baoding. The area of “headstream” in Fig.1 is located near the Mountain area and before the  
156 densely populated areas, thus we considered it is a part of the headstream of FRS. The water  
157 quality in FRS would not change too much during the water transformation in the Mountain area  
158 due to the low anthropogenic activities and wastewater discharge. Therefore, we started our  
159 sampling from the “headstream” area in Fig.1. River water was sampled in three seasons: spring  
160 (May, headstream was not collected), summer (July) and autumn (October) of 2020,  
161 respectively. In order to reduce experimental errors, at least four sample points were randomly  
162 selected in different areas in each sample site, and water samples at each sample point were  
163 taken at two depths:  $\sim 0.1$  m below the water surface (surface samples) and  $\sim 0.3$  m below the  
164 water surface (deep samples). Each sample was collected 150 ml water into a brown  
165 polyethylene bottle, which was acid cleaned and rinsed with surface water before sampling. The  
166 water samples were stored in a cooler with ice bags and then placed in a refrigerator at 4°C after  
167 returning to our laboratory.

### 168 **Pollutant concentration measurement**

169 When water samples were transported to our laboratory, they were filtered using GF/F  
170 filters (Whatman, Kent Great Britain). Then each water sample was separated into 100 ml and 50  
171 ml two parts. The 100 ml water sample was immediately used to determine concentrations of  
172 COD,  $\text{NH}_4^+$ -N and TP by the potassium dichromate method, nesslerization spectrophotometry  
173 and Mo-Sb Anti spectrophotometric method, respectively, according to the procedures of surface  
174 water quality measurements (HJ 828-2017, HJ 535-2009 and GB 11893-89) in China. The other  
175 50 ml water sample was stored with 1.5 ml 68%  $\text{HNO}_3$  at 4°C for the analysis of heavy metal in  
176 two weeks. Pb, Cd and Cr were determined using Atomic Absorption Spectrometry (AAS  
177 ZEE nit-700P). The precision of the instrument was checked through the chemical standards

178 (Merck, Germany) with control blanks yielding a quantitative value of  $100 \pm 4.1\%$  (Rajeshkumar  
179 and Liu, 2018). Five-point calibration curves were used for the concentration measurement, and  
180  $R^2$  values of calibration curves greater than 0.99 were accepted. Two replicates were measured  
181 for each sample, and the heavy metal concentrations in the blanks were subtracted from the  
182 sample values (Xia et al., 2018).

### 183 **Water Pollution Evaluation**

184 Considering the applicability of the evaluation methods, the water quality index ( $WQI$ )  
185 method (Gao et al., 2019; Wang et al., 2017) was used to analyze the comprehensive pollution  
186 conditions of FRS, and the water quality conditions were classified as Table S1.  $WQI$  of  
187 eutrophication ( $WQI_E$ ) was calculated according to Class III water standard (GB3838-2002) due  
188 to it being the present water quality requirement of Baiyangdian; and most of heavy metal  
189 pollutants were lower than Grade III water standard and needed to meet Grade I water standard  
190 as a natural reserve in future (Table S2),  $WQI$  of heavy metals ( $WQI_{HM}$ ) was calculated  
191 according to these two water standards in this study.

192  $WQI$  was computed as follows:

$$193 \quad A_i = \frac{C_i}{C_{si}} \quad (1)$$

$$194 \quad WQI = \frac{1}{n} \sum_{i=1}^n A_i \quad (2)$$

195  $A_i$ —Pollution index of a certain pollutant ( $i$ );

196  $C_i$ —Measured concentration of a certain pollutant ( $i$ );

197  $C_{si}$ —Water quality standard of a certain pollutant;

198  $n$ —Number of elements.

### 199 **Spatiotemporal variation analysis**

200 The remote sensing images of Fuhe River watershed in 2019 growing season were obtained  
201 from Landsat ([www.gscloud.cn](http://www.gscloud.cn)), and then ENVI Classic was used to classify the land use types.  
202 Based on the characteristics of surface feature spectrum and remote sensing image, as well as the  
203 distribution characteristics of the research object, we established training samples for supervised  
204 classification and visual interpretation of land use types with the reference of the national land  
205 use/cover classification system. We continuously optimized the classification results to ensure  
206 the accuracy of the data. After the data of pollutant concentrations in three seasons were  
207 combined with the GPS positioning of each sampling site, Arc-GIS was used to analyze the  
208 spatial and temporal changes of eutrophication and heavy metal pollution in FRS.

### 209 **Data analysis**

210 One-way analysis of variance (ANOVA) was conducted to compare the differences of the  
211 pollution parameters in FRS (least-significance difference, LSD), using SPSS 16.0 for Windows  
212 (SPSS Inc., Chicago, IL, USA, 2002). We checked the normality and homogeneity of variances  
213 for the ANOVAs using Shapiro-Wilk and Levene tests. Data were transformed to meet the  
214 assumptions of normality and homogeneity of variance where necessary. The significance of the  
215 differences among the median values of sampling areas were tested by Kruskal-Wallis One Way  
216 Analysis. Pearson's correlation analysis was used to perform correlations between the eutrophic  
217 parameters and heavy metals (Chen et al., 2021b; Guo et al., 2020). Principal component  
218 analysis (PCA) could explore the possible sources of heavy metals by reducing the  
219 dimensionality of the multivariate water pollutant dataset to 2–3 principle influencing factors,  
220 which commonly occurs in hydrochemistry (Guo et al., 2021; Ismail et al., 2016; Zhuang et al.,

221 2019). In this study, Pearson's correlation analysis and PCA were employed to identify potential  
222 sources and hotspots of heavy metal pollution in FRS. The average values of surface samples and  
223 deep samples in each sample site were used for the Pearson's correlation analysis and PCA. All  
224 the Pearson's correlation and PCA analyses were performed in the R platform (R Core Team,  
225 2018). R package of "FactoMineR" (Lê et al., 2008) was used to calculate the principle  
226 components, and the "factoextra" package (Alboukadel and Fabian, 2017) was used to extract  
227 and visualize the results.

228

## 229 **Results**

### 230 **Extreme pollution in individual sampling site of FRS in three seasons**

231 The changes of eutrophication and heavy metal pollution along the sampling route in FRS  
232 are showed in Fig. 2. Three season average concentrations of eutrophic parameters ( $\text{NH}_4^+\text{-N}$ , TP  
233 and COD) were higher in the sampling sites of out-of-city area and farmland area, whereas, the  
234 higher average concentrations of heavy metals (Pb, Cd and Cr) were concentrated in the out-of-  
235 city city area and town area. Pollution of eutrophication was generally worse than the heavy  
236 metal in FRS (Fig. 2). In spring,  $\text{NH}_4^+\text{-N}$  in F6 and COD in F6, 11 were worse than Class V  
237 water standard (Table S2); the other parameters higher than Class III standard were:  $\text{NH}_4^+\text{-N}$  in  
238 F7, TP in F7-8, COD in F7 and Cd in F8-9, 11, 14. In summer,  $\text{NH}_4^+\text{-N}$  in F5, 7-14 were worse  
239 than Class V standard; the other parameters higher than Class III standard were:  $\text{NH}_4^+\text{-N}$  in F2-  
240 4, TP in F8, 13, COD in F8 and Cd in F9. In autumn,  $\text{NH}_4^+\text{-N}$  in F7, 13-14 and TP in F7, 9 were  
241 worse than Class III water standard. Overall, the pollution hotspots (>Class III standard) in FRS  
242 were mostly (>94%) appeared after the water flowing over the city.

## 243 **Variation of water pollution among different classified areas**

244 Sampling sites in FRS could be classified into five areas: Headstream, City, Towns,  
245 Farmland and Estuary (Fig. 1). There were greatly spatiotemporal changes in each pollution  
246 parameter among these five areas (Fig. 3): (1)  $\text{NH}_4^+\text{-N}$  (average  $4.59\pm 0.15$  and  $0.98\pm 0.04$   $\text{mg}\cdot\text{L}^{-1}$   
247  $^1$ ) and TP (average  $0.14\pm 0.01$  and  $0.11\pm 0.02$   $\text{mg}\cdot\text{L}^{-1}$ ) were all higher in summer and autumn, and  
248 increased dramatically from the city area to the estuary; (2)  $\text{NH}_4^+\text{-N}$  and TP had higher  
249 concentrations in city area in spring; (3) concentrations of COD (average  $42.07\pm 6.93$   $\text{mg}\cdot\text{L}^{-1}$ )  
250 were higher in spring with the severe pollution in the city and farmland areas, whereas, COD in  
251 summer and autumn was higher in the city area; (4) Cd (average  $4.58\pm 0.40$   $\mu\text{g}\cdot\text{L}^{-1}$ ) also showed  
252 higher concentrations in spring than those in summer and autumn in each area in FRS, however  
253 there was no significant temporal variation in Pb and Cr; (5) Pb in spring and summer  
254 ( $16.65\pm 0.85$  and  $13.07\pm 0.39$   $\mu\text{g}\cdot\text{L}^{-1}$ ) was worse than Cd and Cr; and (6) there was no significant  
255 spatial variation in Pb after the headstream, whereas, Cd ( $5.65\pm 1.27$ ,  $2.83\pm 0.64$  and  $2.73\pm 0.32$   
256  $\mu\text{g}\cdot\text{L}^{-1}$ ) and Cr ( $20.00\pm 4.15$ ,  $15.45\pm 2.43$  and  $21.14\pm 3.71$   $\mu\text{g}\cdot\text{L}^{-1}$ ) in the town area in three seasons  
257 were all higher than other places in FRS.

## 258 **Effects of different regions of city on the water pollution in FRS**

259 When water flowed out of the city, Middle River had four significantly highest pollution  
260 parameters among the three rivers:  $\text{NH}_4^+\text{-N}$  and Cd in summer, and  $\text{NH}_4^+\text{-N}$  and Cr in autumn ( $p$   
261 were  $<0.001$ ,  $<0.001$ ,  $<0.001$ , and  $0.007$ ), whereas, North River only had two highest parameters  
262 ( $p$  were  $<0.001$  and  $0.003$ ) and there was none in South River (Table 1). Furtherly, Middle River  
263 had more than 83% of parameters significantly increased when water flowed through the city,  
264 with nearly 5/6 highest increments:  $\text{NH}_4^+\text{-N}$  ( $>6$  times), TP ( $>25$  times), COD ( $>7$  times), Cr ( $>3$

265 times) and Cd (>3 times). Contrastingly, North River had none highest increment, and South  
266 River had one: Pb (>2 times).

### 267 **Relationships among water pollution parameters in FRS**

268 Pearson's correlation analysis showed there were many strongly positive relationships in the  
269 eutrophic parameters and heavy metals (Fig. 4 A). Eutrophic parameters:  $\text{NH}_4^+\text{-N}$  significantly  
270 correlated with TP ( $p=0.0003$ ). Eutrophic parameters and heavy metals:  $\text{NH}_4^+\text{-N}$ , TP and COD  
271 all significantly correlated with Pb ( $p$  were 0.0129, 0.0485 and 0.0044), and COD significantly  
272 correlated with Cd ( $p<0.0001$ ). Principal component analysis (PCA) showed that the first and  
273 second principal components (PCs, denoted as Dims in Fig. 4 B) explained 42.6% and 33% of  
274 the total variance of the heavy metal concentrations in FRS, respectively. Pb and Cd were both  
275 positively associated with PC1 with correlations of 66.6% and 79.2%, and Pb was negatively  
276 associated with PC2 (correlation: -54.9%); Cr was positively associated with PC2 (correlation:  
277 83%), but also partly associated with PC1 with a correlation of 45.4% (Table S3).

### 278 **Water quality assessment: changes of $WQI$ with the distance to Baiyangdian**

279 In spring,  $WQI_E$  mostly exceeded 1.5 in the areas of out-of-city and farmland in FRS (Fig. 5  
280 A), which indicated the water was moderately eutrophic based on Class III water standard in  
281 China (Table S1). In summer and autumn,  $WQI_E$  increased gradually from the headstream to the  
282 estuary area, which both had a significantly negative linear correlation with the distance to the  
283 estuary area ( $p$  were  $<0.001$  and 0.009).  $WQI_E$  in summer significantly increased from about 0.25  
284 (unpolluted level) to around 2.5 (serious pollution) along FRS with a correlation curve slope of  
285 0.027 ( $p < 0.001$ ), which were dramatically higher than those in autumn.

286 Based on Class I water standard,  $WQI_{HM}$  were all higher than 2.0 (moderate pollution,  
287 Table S1) when FRS flowed over the city in spring, and  $WQI_{HM}$  even significantly exceeded 2.5

288 in the middle areas of FRS (Fig. 5 B).  $WQI_{HM}$  showed relative lower values in summer and  
289 autumn compared with spring, with significantly single peak curve patterns from the headstream  
290 to the estuary area ( $p$  were 0.002 and 0.021). The curves increased significantly from about 1.0  
291 (unpolluted level) at both ends of FRS to more than 2.0 around the town area ( $p < 0.001$ ). Based  
292 on Class III water standard,  $WQI_{HM}$  showed similar spatiotemporal variations along FRS, but all  
293 sampling sites were in unpolluted levels (Fig. S1).

294

## 295 Discussion

296 The eutrophication showed an overall improvement in many China's inland waters in recent  
297 decades (Huang et al., 2019; Zhou et al., 2017). However, the nutrient pollutants were not fully  
298 eliminated: the moderate to heavy eutrophication were also found (Guo et al., 2020; Wang et al.,  
299 2017; Wu et al., 2017), and the continuous water quality improvement is needed to effectively  
300 control the water pollution in their inflow rivers (Lv et al., 2020; Wang et al., 2021a; Wang et al.,  
301 2021b; Gao et al., 2021). Our study found a considerable improvement of eutrophication in the  
302 inflow river system of Baiyangdian comparing with previous studies, particularly after the  
303 establishment of Xiongan New Area in 2017. In the city area of FRS,  $NH_4^+$ -N dramatically  
304 decreased from 17.97~36.92 (2009), 11.34 (2013), 13.33~27.18 (2014) and 11.89±1.26 (2017)  
305 to 1.98±0.28  $mg \cdot L^{-1}$  in our study (Fig. 3); TP decreased even more greatly: from 2.34 (2008),  
306 1.53 (2013), 1.23~2.15 (2014), 2.25±0.28 (2015) and 2.90±0.18 (2017) to 0.19±0.04  $mg \cdot L^{-1}$ ;  
307 whereas, COD (17.65±6.89  $mg \cdot L^{-1}$ ) moderately decrease comparing with 33.84±4.47 (2005),  
308 31.4 (2013), 54.63 (2014) and 56.93±10.91  $mg \cdot L^{-1}$  (2017) (Dong et al., 2018; Jia, 2015; Li,  
309 2014; Qiu et al., 2009; Wang et al., 2010). Similar changes of eutrophication were also observed  
310 in town and farmland areas (Dong et al., 2018; Li, 2014; Wang et al., 2010). Eutrophication in

311 the estuary area was not improved so much:  $\text{NH}_4^+\text{-N}$  from 13.20~17.27 (2005-2009) to  
312  $3.51\pm 0.37 \text{ mg}\cdot\text{L}^{-1}$ , TP from 0.34 (2008) to  $0.14\pm 0.01 \text{ mg}\cdot\text{L}^{-1}$  and COD from  $23.13\pm 4.81$  (2005)  
313 to  $13.17\pm 3.20 \text{ mg}\cdot\text{L}^{-1}$  (Qiu et al., 2009; Li et al., 2017; Wang et al., 2010). However, the  
314 eutrophic parameters in nearly half of the sample sites in FRS still did not reach the present  
315 water quality requirement of Baiyangdian (Class III water standard, Fig. 3), and the  $\text{NH}_4^+\text{-N}$  and  
316 TP in summer and COD in spring in FRS were all higher than those in Baiyangdian (Li et al.,  
317 2021b; Meng et al., 2021; Zhao et al., 2020), which were great threats to the water quality of  
318 Baiyangdian (Table S2). In addition, the seriously eutrophic parameters were also observed in  
319 many sampling sites, particularly, the  $\text{NH}_4^+\text{-N}$  and COD in spring and the  $\text{NH}_4^+\text{-N}$  in summer  
320 significantly exceeded the Class V water standard in some hotspots ( $p<0.001$ , Fig. 2), which  
321 may have tremendous influences on the water quality of the whole FRS and Baiyangdian. Thus,  
322 eutrophication, especially  $\text{NH}_4^+\text{-N}$  and COD, did not improved in the whole FRS, and the current  
323 water quality treatments in Baiyangdian watershed only alleviated the eutrophic pollution in  
324 FRS. Furthermore, the eutrophication of Baiyangdian needed to be greatly improved to meet the  
325 higher water quality requirement as a natural reserve (Class I water standard, Table S2). All  
326 these demonstrated that more precise pollution remediations are needed to deal with the  
327 eutrophic pollutants in FRS in the future.

328 Water pollution caused by heavy metals has caused widespread concern due to their health  
329 effects on aquatic animals and humans (Ismail et al., 2016; Rajeshkumar and Li, 2018; Zhang et  
330 al., 2017). Whereas, many previous studies only concerned the eutrophication in the water of  
331 FRS and Baiyangdian (Jia, 2015; Li et al., 2021b; Liang et al., 2017; Zhao et al., 2020), and only  
332 one research has reported the pollution of heavy metals in the estuary area of FRS: Pb ( $0.91$   
333  $\mu\text{g}\cdot\text{L}^{-1}$ ), Cd ( $0.08 \mu\text{g}\cdot\text{L}^{-1}$ ) and Cr ( $3.75 \mu\text{g}\cdot\text{L}^{-1}$ ) in summer of 2016 (Gao et al., 2019). Our study

334 showed that the pollution of heavy metal in FRS was much better than the eutrophic pollution:  
335 heavy metals in many sampling sites have nearly reached the Class I water standard (Fig. 3).  
336 The average concentrations of Pb, Cd and Cr in FRS stayed in a relative moderate level  
337 compared with other aquatic systems globally. In the Dan River drainage, the average  
338 concentrations of Cr and Cd were 0.10 and 0.70  $\mu\text{g}\cdot\text{L}^{-1}$  (Meng et al., 2016), which were  
339 dramatically lower than we found in FRS. Heavy metal pollution in rivers of Greece increased  
340 from 1999 to 2019, however, the recent contents of Pb, Cd and Cr were still comparable to the  
341 concentrations in FRS (Karaouzas et al., 2021). Whereas, in Houjing River of Taiwan, the  
342 average concentrations of Pb, Cd and Cr were 569, 8 and 96  $\mu\text{g}\cdot\text{L}^{-1}$  (Vu et al., 2017), in which Pb  
343 and Cr were significantly higher than those in FRS. In Huaihe River, the average Pb, Cd and Cr  
344 concentrations were 155.60, 69.54 and 22.13  $\mu\text{g}\cdot\text{L}^{-1}$  (Wang et al., 2017), and Pb and Cd were  
345 significantly higher than Class V water standard and also dramatically higher than what we  
346 found in FRS. Furthermore, the similar concentration distributions of heavy metals could  
347 indicate the long-distance transportation of heavy metals from the inflow rivers to the  
348 downstream lakes (Guo et al., 2020; Meng et al., 2016). Our results displayed the mobility and  
349 influence of heavy metals in FRS to the water of Baiyangdian (Fig. 3): the concentrations of  
350 heavy metals Cr, Cd and Pb in FRS showed the similar concentration distributions but were all  
351 significantly higher than those in water of Baiyangdian (Gao et al., 2019; Meng et al., 2021;  
352 Zhao et al., 2020). The inflow rivers could collect heavy metals from the whole watershed and  
353 severely contaminate themselves and downstream lakes (Guo et al., 2020; Meng et al., 2016; Lv  
354 et al., 2020). Therefore, in order to completely ameliorate the pollution of heavy metals in  
355 Baiyangdian, the sources and routes of heavy metals entering the inflow rivers should be  
356 concerned and eliminated.

357 We did not find any previous study that has shown the spatiotemporal pattern of water  
358 pollution in FRS, whereas, the present study displayed dramatically spatial and temporal  
359 variations of eutrophication and heavy metal pollution (Fig. 2, 3 and 5), which were consistent  
360 with other aquatic ecosystems (Chen et al., 2021b; Guo et al., 2020; Wang et al., 2021a). The  
361 captured spatiotemporal patterns would allow us to identify the pollution hotspots and seriously  
362 polluted periods in FRS. The eutrophication in FRS showed that  $\text{NH}_4^+\text{-N}$  and TP increased  
363 significantly from the city area to the estuary area in summer and autumn, and  $\text{NH}_4^+\text{-N}$  and TP in  
364 these two seasons were all higher than those in spring (Fig. 3), which could be mainly due to the  
365 domestic sewage (Li et al., 2017; Wang et al., 2017) and runoffs from intensive agricultural  
366 activities (Tao et al., 2020; Wang et al., 2017). Whereas, COD contents in spring were higher  
367 than those in summer and autumn in FRS, which may be caused by the deteriorated stagnant  
368 wastewater and sediment release due to the low flow rate of FRS in spring (Ni, et al., 2016; Piao  
369 et al., 2010; Zhu et al., 2019). Regarding water quality assessment,  $WQI_E$  revealed pollution  
370 hotspots around the middle area of FRS in spring, and  $WQI_E$  in summer and autumn linearly  
371 increased from unpolluted levels to serious pollution along FRS, showing the pollution hotspots  
372 in these two seasons were in farmland and estuary areas (Fig. 5 A). The seriously eutrophic water  
373 accumulated in the end of FRS could directly enter Baiyangdian and cause contamination, which  
374 demonstrated a great influence of inflow rivers' eutrophic pollutants to the eutrophication in  
375 lakes. In contrast to eutrophication, different spatiotemporal variations of the heavy metals were  
376 observed in FRS. The contents of Pb were mostly higher than Cd and Cr but without clear spatial  
377 variations in FRS (Fig. 3), which indicated Pb could be mainly originated from a constantly line  
378 sources along FRS—traffic pollution (Ewen et al., 2009; Vu et al., 2017). Whereas, Cd and Cr in  
379 the town area were all higher than other places in three seasons, which indicated Cd and Cr were

380 likely due to the release from historical polluted sediments in the town area (Peng et al., 2009;  
381 Vu et al., 2017) or the industrial wastewater in the town and city areas (Chen et al., 2021a; Li et  
382 al., 2021a). The higher concentrations of Cd in spring additionally confirmed that Cd pollution  
383 was tremendously influenced by the accumulation effect in stagnant water originating from  
384 sediments (Meng et al., 2016; Peng et al., 2009; Wang et al., 2017).  $WQI_{HM}$  showed single peak  
385 curves along FRS, and increased significantly from unpolluted levels at both ends of FRS to the  
386 highest level of pollution just after the city area (around the town area), furtherly demonstrating  
387 the pollution hotspots of heavy metals were caused by the sources in the high population density  
388 regions (Fig. 5 B). Meanwhile, different regions in the city area also greatly affected the water  
389 quality of FRS (Table 1): the water flowing through the middle of city was seriously polluted,  
390 whereas, the waters flowing through the edges of the city were only slightly polluted. Overall,  
391 these spatiotemporal distribution characteristics above clearly clarified the varied pollution  
392 hotspots, the seriously polluted periods and the potential sources in FRS. Water quality  
393 managements in the future should take serious considerations of these weak parts in current  
394 pollution treatments, and formulate and conduct spatiotemporally flexible treatments based on  
395 this study to furtherly improve water quality in the Baiyangdian watershed.

396 Trace elements exhibiting high correlations may share similar analogous behaviors during  
397 transformation and migration (Ke et al., 2017; Wang et al., 2017), which can suggest their  
398 potential sources and pathways in the water environment (Chen et al., 2021b; Guo et al., 2020;  
399 Ke et al., 2017). Pearson's correlation showed  $NH_4^+-N$ , TP and COD all significantly correlated  
400 with Pb ( $p$  were 0.0129, 0.0485 and 0.0044) and COD significantly correlated with Cd  
401 ( $p < 0.0001$ , Fig. 4 A), indicating Pb, Cd and eutrophic pollutants were likely originated from  
402 similar sources in FRS, such as inflows from domestic sewage and traffic activities (Chen et al.,

403 2021b; Ewen et al., 2009; Guo et al., 2021), runoff from intensive applications of fertilizers and  
404 pesticides (Wang et al., 2017; Xia et al., 2018) and release from historical polluted sediments (Ni  
405 et al., 2016; Peng et al., 2009; Zhu et al., 2019). PCA showed that Pb was positively associated  
406 with PC1 but negatively associated with PC2 (Table S3), which furtherly indicated Pb in FRS  
407 could be attributed to the sources of traffic pollution, agricultural practices and historical polluted  
408 sediments rather than industrial wastewater discharges (Ewen et al., 2009; Wang et al., 2017).  
409 This is consistent with the finding in the spatiotemporal analysis that Pb could be originated from  
410 a constantly line sources along FRS (Fig. 3). Cd was also positively associated with PC1,  
411 confirming Pb and Cd have similar hydro-chemical characteristics and common sources in the  
412 water of FRS (Chen et al., 2021b; Zhuang et al., 2019). In addition, Cd significantly correlated  
413 with COD, which could more accurately attribute Cd pollution to the agricultural practices and  
414 polluted sediments as COD. In contrast to Pb and Cd, Cr positively associated with PC2 but also  
415 partly associated with PC1, which thus can attribute Cr to the sources of sewage releases from  
416 industrial activities and polluted sediments (Peng et al., 2009; Vu et al., 2017). All heavy metals  
417 partly attributed to the historical polluted sediments were consistent with the results that the  
418  $WQI_{HM}$  were relatively higher in the stagnant water in spring (Fig. 5 B). Industrial wastewater  
419 was imported into Baiyangdian water system since the 1980s, which caused two-thirds of this  
420 region to be contaminated and a large amount of pollution has accumulated in the sediments  
421 (Zhang et al., 2018; Zhu et al., 2019). Heavy metals released from these sediments could cause a  
422 long-term threat to the water quality and aquatic biota health in this region (Ismail et al., 2016;  
423 Ke et al., 2017; Rajeshkumar and Li, 2018).

424 With environmental remediations and increased government financed investments, the  
425 water quality (particularly eutrophication) in Chinese inland waters was improved markedly over

426 recent decades (Huang et al., 2019; Zhou et al., 2017; Zhuang et al., 2019). However, in order to  
427 completely mitigate the water pollution from Chinese inland waters (include Baiyangdian  
428 watershed) in next decades, the importance of controlling the inflow river pollution and  
429 understanding its spatiotemporal variations was gradually recognized (He et al., 2020; Tong et  
430 al., 2017). We should deeply understand about the pollution sources of inland waters, the main  
431 pollutants deteriorating the water quality and the spatiotemporal variations of these pollutants  
432 (Huang et al., 2018; He et al., 2020; Wang et al., 2021a). Then, more effective water pollution  
433 treatments can be taken with focalizations to reduce the pollution from industrial activities,  
434 traffic pollution and agricultural practices, as well as the remediation of polluted sediments. For  
435 instance, specific constructed wetlands could be built based on this information for the water  
436 quality restoration of the targeted area and pollutants. Therefore, the spatiotemporal changes of  
437 the water pollution showed in this study, including the pollution hotspots, serious periods and  
438 potential sources, provided important scientific basis for making effective and flexible water  
439 quality treatments in the whole watershed of Baiyangdian.

440

## 441 **Conclusions**

442 Our study demonstrated a considerable improvement of the eutrophication and a good  
443 condition of the heavy metals in the water of FRS after the establishment of Xiongan New Area.  
444 However, the eutrophic parameters in nearly half of the sites in FRS still did not reach the  
445 present water quality requirement of Baiyangdian, and the heavy metals were mostly associated  
446 with traffic pollution, agricultural practices and historical polluted sediments, which were not  
447 easily to be controlled and eliminated. In addition, dramatically spatiotemporal changes of  
448 pollution in FRS were found in this study, allowing the conclusions: the eutrophication was

449 highest in summer, and the severely eutrophic pollution concentrated around the estuary area;  
450 whereas, the pollution of heavy metals was relatively similar among three seasons with the  
451 prominent pollution around the town area. The serious contamination in these varied pollution  
452 hotspots and periods in FRS may have tremendous influences on the water quality of the  
453 downstream Baiyangdian. All these findings revealed the weak parts in current pollution  
454 treatments, and provided scientific basis for conducting more precise water quality managements  
455 to fully eradicate the water pollutants in future.

456

## 457 **Acknowledgements**

458 We are very grateful for some data support provided by Environmental Protection Bureau  
459 of Baoding City. The authors would like to thank the editors, the reviewer of Kiran Liversage,  
460 and the other two anonymous reviewers for their valuable comments and suggestions on this  
461 paper.

462

## 463 **References**

- 464 Aubriot, L.B., Zabaleta, F., Bordet, D., Sienna, J., Risso, M., Achkar, M., and Somma, A., 2020. Assessing the  
465 origin of a massive cyanobacterial bloom in the Rio de la Plata (2019): Towards an early warning system.  
466 *Water Research*. 181, 115944. <https://doi.org/10.1016/j.watres.2020.115944>
- 467 Alboukadel, K., Fabian, M., 2017. factoeextra: Extract and Visualize the Results of Multivariate Data Analyses.  
468 <http://www.sthda.com/english/rpkgs/factoeextra> (accessed 1 April 2020).
- 469 Chen, J.Q., Chen, M.L., Zhang, X.B., Yang, T.W., An, S.Q., Zhang, Y.B., Fu, H.F., 2020. The Restoration Project  
470 of Fuhe River Estuarine Wetland in Xiong'an New Area. *Wetland Science & Managment*. 16, 4-8 [in  
471 Chinese]. <https://doi.org/10.3969/j.issn.1673-3290.2020.04.01>
- 472 Chen P., Fu, C.F., Ji, X.G., Kang, G.Q., 2021a. Study on the Ecological effects of Optimization Scheme for Water  
473 Quality Implement in Baiyangdian. *Journal of Hydroecology*. 1-11 [in Chinese].

- 474 <https://doi.org/10.15928/j.1674-3075.202005250148>
- 475 Chen, S., Wang, S.M., Yu, Y.X., Dong, M.J., Li, Y.Q., 2021b. Temporal trends and source apportionment of water  
476 pollution in Honghu Lake, China. *Environ Sci Pollut Res Int.* 28, 60130-60144.
- 477 Cheng, W.Q., Bo, Q.Y., Sun, T., 2018. Baiyangdian environmental and ecological changes and impact on the  
478 construction of Xiongan New Area. *Forestry and Ecological Sciences.* 33, 113-120 [in Chinese].  
479 <https://doi.org/10.13320/j.cnki.hifor.2018.0018>
- 480 Dong, Y.H., 2018. Study on purification effect of aquatic plants on water quality of Fuhe River in Baoding City  
481 (Thesis). Baoding, Hebei Agricultural University [in Chinese].
- 482 Ewen, C., Anagnostopoulou, M.A., Ward, N.I., 2009. Monitoring of heavy metal levels in roadside dusts of  
483 Thessaloniki, Greece in relation to motor vehicle traffic density and flow. *Environ. Monit. Assess.* 157,  
484 483-498. <https://doi.org/10.1007/s10661-008-0550-9>
- 485 Gao, Q.S., Tian, Z.Q., Jiao, L.X., Ding, L., Yang, S.W., He, Z.F., Cui, Z.D., Jia, H.B., 2019. Pollution  
486 characteristics and ecological risk assessment of heavy metals in Baiyangdian Lake. *Journal of  
487 Environmental Engineering Technology.* 9, 66-75 [in Chinese]. <https://doi.org/10.3969/j.issn.1674-991X.2019.01.010>
- 488
- 489 Gao, K.W., Zhu, Y.Y., Sun, F.H., Chen, Y.Q., Liao, H.Q., Ma, H.H., Hu, X.Y., 2021. A study on the collaborative  
490 control of water quality of nitrogen and phosphorus between typical lakes and their inflow rivers in China.  
491 *Journal of Lake Sciences.* 33, 1400-1414. [in Chinese].
- 492 Guo, W., Huo, S.L., Ding, W.J., 2015. Historical record of human impact in a lake of northern China: Magnetic  
493 susceptibility, nutrients, heavy metals and OCPs. *Ecol Indic.* 57, 74-81.  
494 <http://dx.doi.org/10.1016/j.ecolind.2015.04.019>
- 495 Guo, C.B., Chen, Y.S., Xia, W.T., Qu, X., Yuan, H., Xie, S.G., Lin, L.S., 2020. Eutrophication and heavy metal  
496 pollution patterns in the water supplying lakes of China's south-to-north water diversion project. *Sci. Total  
497 Environ.* 711, 134543. <https://doi.org/10.1016/j.scitotenv.2019.134543>
- 498 Guo, S., Zhang, Y.Z., Xiao, J.Y., Zhang, Q.Y., Ling, J.H., Chang, B.J., Zhao, G.L., 2021. Assessment of heavy  
499 metal content, distribution, and sources in Nansi Lake sediments, China. *Environ Sci Pollut Res Int.* 28,  
500 30929-30942.

- 501 He, J., Wu, X., Zhang, Y., Zheng, B.H., Meng, D., Zhou, H.B., Lu, L., Deng, W.M., Shao, Z., and Qin, Y.H., 2020.  
502 Management of water quality targets based on river-lake water quality response relationships for lake  
503 basins - A case study of Dianchi Lake. *Environ Res.* 186, 109479.  
504 <https://doi.org/10.1016/j.envres.2020.109479>
- 505 Huang, J.C., Zhang, Y.J., Huang, Q., and Gao, J.F., 2018. When and where to reduce nutrient for controlling  
506 harmful algal blooms in large eutrophic lake Chaohu, China? *Ecological Indicators.* 89, 808-817.
- 507 Huang, J.C., Zhang, Y.J., Arhonditsis, G.B., Gao, J.F., Chen, Q.W., Wu, N.C., Dong, F.F., Shi, W.Q., 2019. How  
508 successful are the restoration efforts of China's lakes and reservoirs? *Environ Int.* 123, 96-103.  
509 <https://doi.org/10.1016/j.envint.2018.11.048>
- 510 Ismail, A., Toriman, M.E., Juahir, H., Zain, S.M., Habir, N.L.A., Retnam, A., Kamaruddin, M.K.A., Umar, R., Azid,  
511 A., 2016. Spatial assessment and source identification of heavy metals pollution in surface water using  
512 several chemometric techniques. *Mar. Pollut. Bull.* 106, 292-300.  
513 <https://doi.org/10.1016/j.marpolbul.2015.10.019>
- 514 Jia, L.F., 2015. The study on typical pollution factors change rule and water quality assessment of Baodingfu river  
515 (Thesis). Baoding, Hebei Agricultural University [in Chinese].
- 516 Karaouzas, I., Kapetanaki, N., Mentzafou, A., Kanellopoulos, T.D., Skoulikidis, N., 2021. Heavy metal  
517 contamination status in Greek surface waters: A review with application and evaluation of pollution indices.  
518 *Chemosphere.* 263, 128192. <https://doi.org/10.1016/j.chemosphere.2020.128192>
- 519 Ke, X., Gui, S.F., Huang, H., Zhang, H.J., Wang, C.Y., Guo, W., 2017. Ecological risk assessment and source  
520 identification for heavy metals in surface sediment from the Liaohe River protected area, China.  
521 *Chemosphere.* 175, 473-481. <https://doi.org/10.1016/j.chemosphere.2017.02.029>
- 522 Lê, S., Josse, J., Husson, F., 2008. FactoMineR: An R Package for Multivariate Analysis. *Journal of Statistical*  
523 *Software.* <https://doi.org/10.18637/jss.v025.i01>.
- 524 Li, Y., 2014. Study on change rule of pollution factors and prediction model of the NH<sub>4</sub><sup>+</sup>-N concentration of Fu  
525 River (Thesis). Baoding, Hebei Agricultural University [in Chinese].
- 526 Li, C.H., Zheng, X.K., Zhao, F., Wang, X., Cai, Y.P., Zhang, N., 2017. Effects of Urban Non-Point Source Pollution  
527 from Baoding City on Baiyangdian Lake, China. *Water* 9. <https://doi.org/10.3390/w9040249>
- 528 Li, Y.Z., Chen, H.Y., Sun, W.C., 2021a. Load estimation and source apportionment of nitrogen, phosphorus and

- 529 COD in the basin of Lake Baiyang. *China Environmental Science*. 41, 366-376 [in Chinese].  
530 <https://doi.org/10.19674/j.cnki.issn1000-6923.2021.0042>
- 531 Li, L.Q., Chen, X.H., Zhang, M.Y., Zhang, W.J., Wang, D.S., Wang, H.J., 2021b. The spatial variations of water  
532 quality and effects of water landscape in Baiyangdian Lake, North China. *Environ Sci Pollut Res Int*.  
533 <https://doi.org/10.1007/s11356-021-16938-0>
- 534 Liang, H.Y., Zhai, D.Q., Kong, X.L., Yuan, R.Q., Wang, S.Q., 2017. Sources, migration and transformation of  
535 nitrate in Fuhe River and Baiyangdian Lake, China. *Chinese Journal of Eco-Agriculture*. 25, 1236-1244 [in  
536 Chinese]. <https://doi.org/10.13930/j.cnki.cjea.161187>
- 537 Lv, W., Yang, H., Yang J.Y., Ma, Q., Gao, X.P., Jiang, R.D., Wang, X.J., Xu, Y., Nie, Q., 2020. Relationship  
538 between water quality in Lake Taihu and pollutant fluxes of the rivers surrounding Lake Taihu in Jiangsu  
539 Province. *Journal of Lake Sciences*. 32: 1454-1462. [in Chinese].
- 540 Meng, Q.P., Zhang, J., Zhang, Z.Y., Wu, T.R., 2016. Geochemistry of dissolved trace elements and heavy metals in  
541 the Dan River Drainage (China): distribution, sources, and water quality assessment. *Environ. Sci. Pollut.*  
542 *Res.* 23, 8091-8103. <https://doi.org/10.1007/s11356-016-6074-x>
- 543 Meng, X., Zhang, W.Q., and Shan, B.Q., 2021. Evaluating the biotoxicity of surface water in a grassy lake in North  
544 China. *J Environ Sci*. 102, 316-325.
- 545 Ni, Z.K., Wang, S.R., Wang, Y.M., 2016. Characteristics of bioavailable organic phosphorus in sediment and its  
546 contribution to lake eutrophication in China. *Environ. Pollut.* 219, 537-544.  
547 <https://doi.org/10.1016/j.envpol.2016.05.087>
- 548 Peng, J.F., Song, Y.H., Yuan, P., Cui, X.Y., Qiu, G.L., 2009. The remediation of heavy metals contaminated  
549 sediment. *J. Hazard. Mater.* 161, 633-640. <https://doi.org/10.1016/j.jhazmat.2008.04.061>
- 550 Piao, S.L., Ciais, P., Huang, Y., Shen, Z.H., Peng, S.S., Li, J.S., Zhou, L.P., Liu, H.Y., Ma, Y.C., Ding, Y.H.,  
551 Friedlingstein, P., Liu, C.Z., Tan, K., Yu, Y.Q., Zhang, T.Y., Fang, J.Y., 2010. The impacts of climate  
552 change on water resources and agriculture in China. *Nature*. 467, 43-51.  
553 <https://doi.org/10.1038/nature09364>
- 554 Qiu, R.Z., Li, Y.X., Yang, Z.F., Shi, J.H., 2009. Influence of water quality change in Fu River on Wetland  
555 Baiyangdian. *Front. Earth Sci*. 3, 397. <https://doi.org/10.1007/s11707-009-0056-y>

- 556 R Core Team, 2018. R: A Language and Environment for Statistical Computing. R Foundation for Statistical  
557 Computing, Vienna. <https://www.R-project.org>.
- 558 Rajeshkumar, S., Li, X., 2018. Bioaccumulation of heavy metals in fish species from the Meiliang Bay, Taihu Lake,  
559 China. *Toxicol Rep.* 5, 288-295. <https://doi.org/10.1016/j.toxrep.2018.01.007>
- 560 Sinha, E., Michalak, A.M., and Balaji, V., 2017. Eutrophication will increase during the 21st century as a result of  
561 precipitation changes. *Science.* 357, 405–408.
- 562 Tao, Y., Liu, J., Guan, X.Y., Chen, H.R., Ren, X.Q., Wang, S.L., Ji, M.Z., 2020. Estimation of potential agricultural  
563 non-point source pollution for Baiyangdian Basin, China, under different environment protection policies.  
564 *Plos One* 15, e0239006. <https://doi.org/10.1371/journal.pone.0239006>
- 565 Tong, Y.D., Zhang, W., Wang, X.J., Couture, R.M., Larssen, T., Zhao, Y., Li, J., Liang, H.J., Liu, X.Y., Bu, X.G.,  
566 He, W., Zhang, Q.G., and Lin, Y., 2017. Decline in Chinese lake phosphorus concentration accompanied  
567 by shift in sources since 2006. *Nature Geoscience.* 10, 507-511.
- 568 Vu, C.T., Lin, C., Shern, C.C., Yeh, G., Le, V.G., Tran, H.T., 2017. Contamination, ecological risk and source  
569 apportionment of heavy metals in sediments and water of a contaminated river in Taiwan. *Ecol. Indic.* 82,  
570 32-42. <https://doi.org/10.1016/j.ecolind.2017.06.008>
- 571 Wang, J., Gao, G., Pei, Y.S., Yang, Z.F., 2010. Sources and transformations of nitrogen in the Fuhe River of the  
572 Baiyangdian Lake. *Environmental Science.* 31, 2905-2910 [in Chinese].  
573 <https://doi.org/10.13227/j.hjlx.2010.12.035>
- 574 Wang, J., Liu, G.J., Liu, H.Q., Lam, P.K.S., 2017. Multivariate statistical evaluation of dissolved trace elements and  
575 a water quality assessment in the middle reaches of Huaihe River, Anhui, China. *Sci. Total. Environ.* 583,  
576 421-431. <https://doi.org/10.1016/j.scitotenv.2017.01.088>
- 577 Wang, J.H., Li, C., Xu, Y.P., Li, S.Y., Du, J.S., Han, Y.P., and Hu, H.Y., 2021a. Identifying major contributors to  
578 algal blooms in Lake Dianchi by analyzing river-lake water quality correlations in the watershed. *Journal of*  
579 *Cleaner Production.* 315, 128144. <https://doi.org/10.1016/j.jclepro.2021.128144>
- 580 Wang, W.D., Yang, T., Guan, W.B., Peng, W.X., Wu, P., Zhong, B., Zhou, C.D., Chen, Q.H., Zhang, R.B., Xu, K.,  
581 and Yin, C.Q., 2021b. Ecological wetland paradigm drives water source improvement in the stream  
582 network of Yangtze River Delta. *Journal of Environmental Sciences.* 110, 55-72.
- 583 Wu, Z.S., Zhang, D.W., Cai, Y.J., Wang, X.L., Zhang, L., Chen, Y.W., 2017. Water quality assessment based on the

- 584 water quality index method in Lake Poyang: The largest freshwater lake in China. *Sci Rep.* 7, 17999.  
585 <https://doi.org/10.1038/s41598-017-18285-y>
- 586 Xia, J., Zhang, Y.Y., 2017. Water resource and pollution safeguard for Xiong'an New Area construction and its  
587 sustainable development, China academic journal electronic publishing house. *Bulletin of the Chinese  
588 Academy of Sciences.* 32, 1199-1205 [in Chinese]. <https://doi.org/10.16418/j.issn.1000-3045.2017.11.004>
- 589 Xia, W.T., Qu, X., Zhang, Y.X., Wang, R., Xin, W., Guo, C.B., Bowker, J., Chen, Y.S., 2018. Effects of  
590 Aquaculture on Lakes in the Central Yangtze River Basin, China, III: Heavy Metals. *N. Am. J. Aquacult.*  
591 80, 436-446. <https://doi.org/10.1002/naaq.10060>
- 592 Yi, Y.J., Lin, C.Q., Tang, C.H., 2020. Hydrology, environment and ecological evolution of Lake Baiyangdian since  
593 1960s. *J. Lake Sci.* 32, 1333-1347 (in Chinese). <https://doi.org/10.18307/2020.0500>
- 594 Zha, H.M., Zhu, M.Y., Zhu, G.W., Yang, Z.S., Xu, H., Shen, R.J., Zhong, C.N., 2018. Seasonal Difference in Water  
595 Quality Between Lake and Inflow/Outflow Rivers of Lake Taihu, China. *Environmental Science.* 39,  
596 1102-1112. [in Chinese]. DOI: 10.13227/j.hjxk.201707184
- 597 Zhang, Y., Liu, Y.Y., Niu, Z.G., Jin, S.P., 2017. Ecological risk assessment of toxic organic pollutant and heavy  
598 metals in water and sediment from a landscape lake in Tianjin City, China. *Environ. Sci. Pollut. Res. Int.* 24,  
599 12301-12311. <https://doi.org/10.1007/s11356-017-8906-8>
- 600 Zhang, C., Shan, B.Q., Zhao, Y., Song, Z.X., Tang, W.Z., 2018. Spatial distribution, fractionation, toxicity and risk  
601 assessment of surface sediments from the Baiyangdian Lake in northern China. *Ecol. Indic.* 90, 633-642.  
602 <https://doi.org/10.1016/j.ecolind.2018.03.078>
- 603 Zhang, R.Q., Wu, F.C., Giesy, J.P., 2019. Tissue-based assessment of hazard posed by mercury and selenium to  
604 wild fishes in two shallow Chinese lakes. *Environmental Science and Pollution Research.* 26, 15989-15999.
- 605 Zhao, Y.L., Wang, S.L., Zhang, F.F., Shen, Q., Li, J.S., Yang, F., 2021. Remote Sensing-Based Analysis of Spatial  
606 and Temporal Water Colour Variations in Baiyangdian Lake after the Establishment of the Xiong'an New  
607 Area. *Remote Sens.* 13, 1729. <https://doi.org/10.3390/rs13091729>
- 608 Zhao, Q.W., Wang, J.Z., Wei, H., Li, J.T., Zhang, Y.M., 2020. Variation characteristics of nitrogen, phosphorus and  
609 heavy metals in waters from Baiyangdian Lake and the influencing factors. *Journal of Water Resources &  
610 Water Engineering.* 31, 103-108 [in Chinese]. <https://doi.org/10.11705/j.issn.1672-643X.2020.06.16>
- 611 Zhou, Y.Q., Ma, J.R., Zhang, Y.L., Qin, B.Q., Jeppesen, E., Shi, K., Brookes, J.D., Spencer, R.G.M., Zhu, G.W.,

612 Gao, G., 2017. Improving water quality in China: Environmental investment pays dividends. *Water Res.*  
613 118, 152-159. <https://doi.org/10.1016/j.watres.2017.04.035>

614 Zhu, Y.Y., Jin, X., Tang, W.Z., Meng, X., and Shan, B.Q., 2019. Comprehensive analysis of nitrogen distributions  
615 and ammonia nitrogen release fluxes in the sediments of Baiyangdian Lake, China. *J Environ Sci (China)*.  
616 76, 319-328.

617 Zhuang, W., Ying, S.C., Frie, A.L., Wang, Q., Song, J.M., Liu, Y.X., Chen, Q., Lai, X.Y., 2019. Distribution,  
618 pollution status, and source apportionment of trace metals in lake sediments under the influence of the  
619 South-to-North Water Transfer Project, China. *Sci. Total Environ.* 671, 108-118.  
620 <https://doi.org/10.1016/j.scitotenv.2019.03.306>

621

# Figure 1

Distribution of sampling sites in one of inflow river systems of Baiyangdian–Fuhe river system (FRS)

Sampling sites in FRS were classified into 5 areas according to their different positions and surrounding land-use conditions along the sampling route: Headstream (F1-3), City (F4-8), Towns (F9-10), Farmland (F11-13) and Estuary (F14).

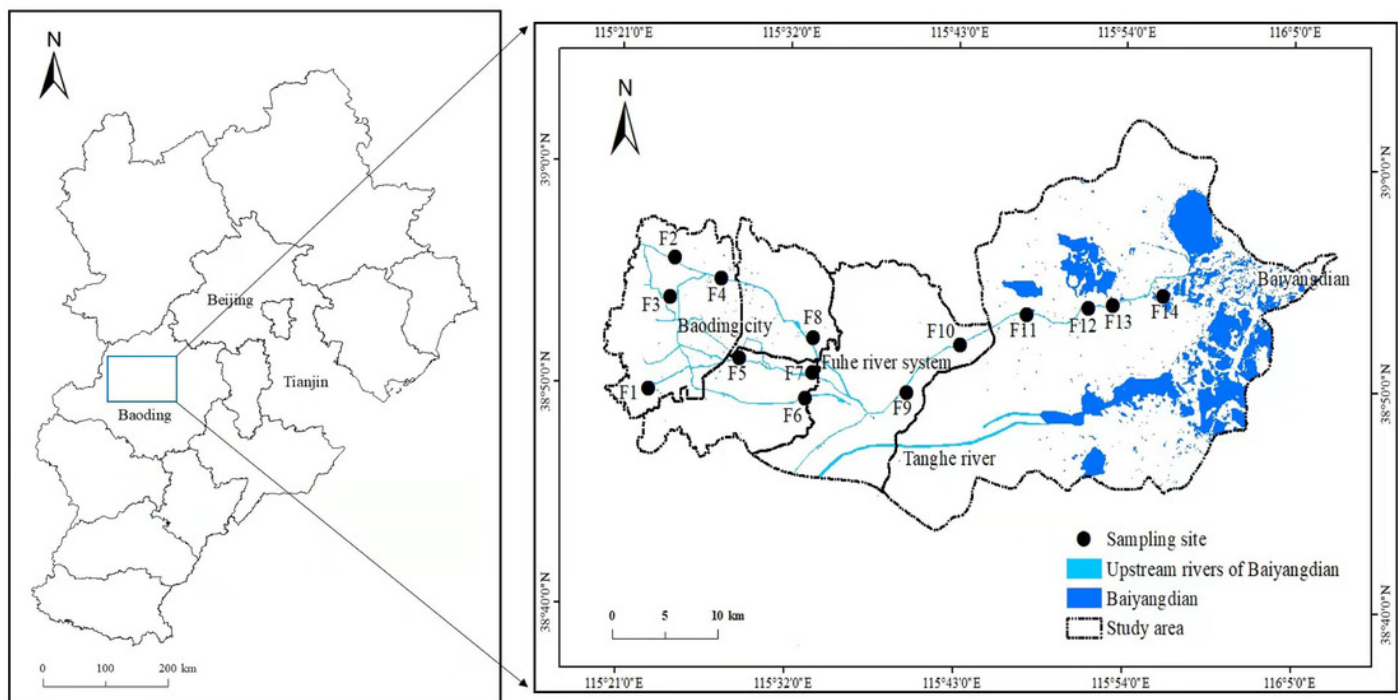


## Figure 2

Distributions of average concentration of each water pollution parameter in three seasons in FRS:  $\text{NH}_4^+$ -N (A), TP (B), COD (C), Pb (D), Cd (E), Cr (F)

The size of pie chart in each sampling site indicated the average concentration of each pollution parameter of three seasons, and different colors in the pie chart indicated the contributions of different seasons to the average concentration of individual pollution parameter.

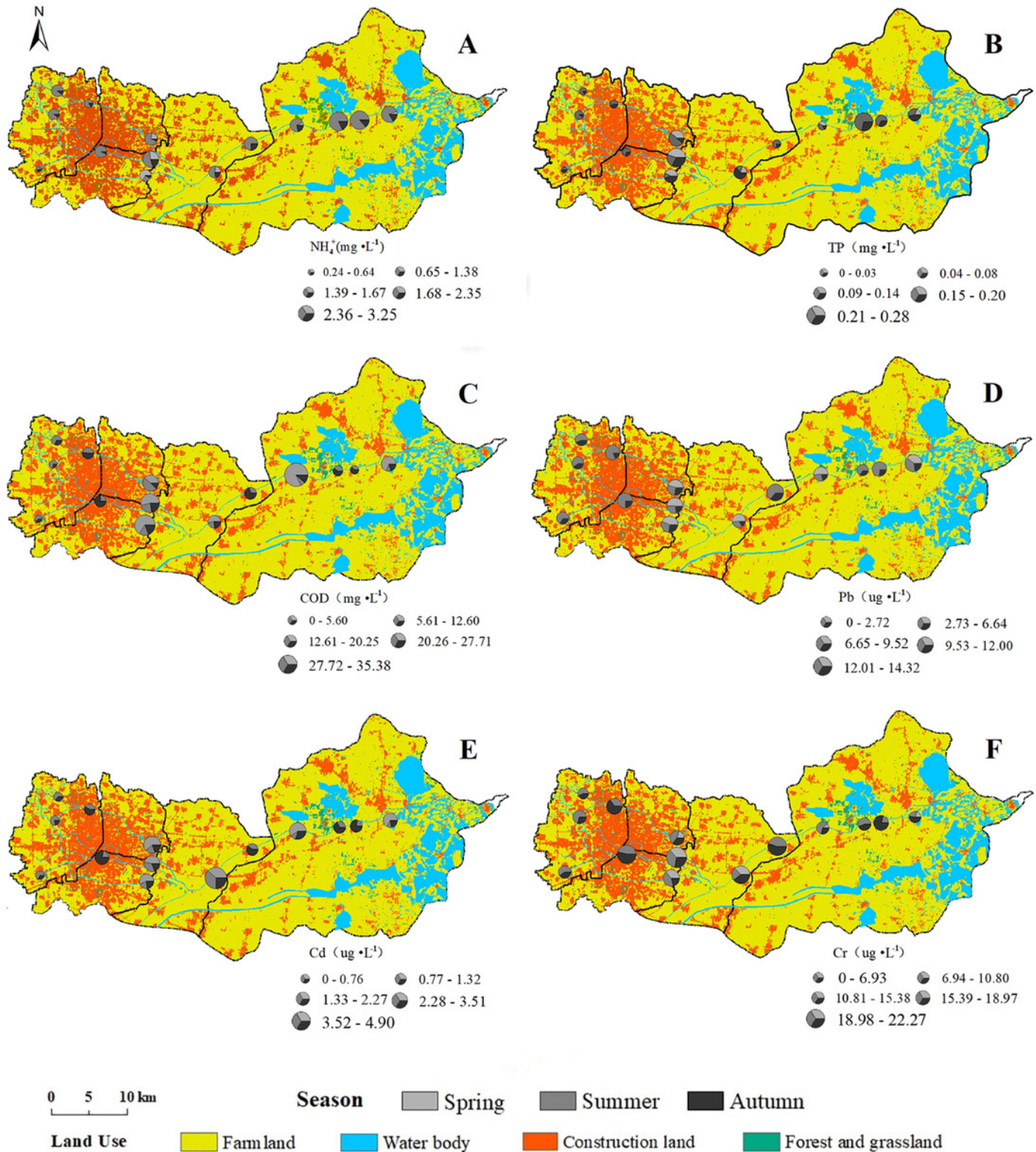


## Figure 3

Distributions of individual water pollution parameters in different areas of FRS in three seasons

In each graph, solid line indicated Class III surface water quality standard, and dash line indicated Class I surface water quality standard in China (Table S2). Box plots indicated median and first and third quartiles, with whiskers extending to the farthest values within 1.5 times the upper and lower quartiles. Outliers beyond this range were shown as points. The significance of the differences among the median values of sampling areas were indicated by the “\*\*” and “\*” in the graph at the level p-values of  $<0.01$  and  $<0.05$ , respectively. Sample size  $N \geq 8$ .

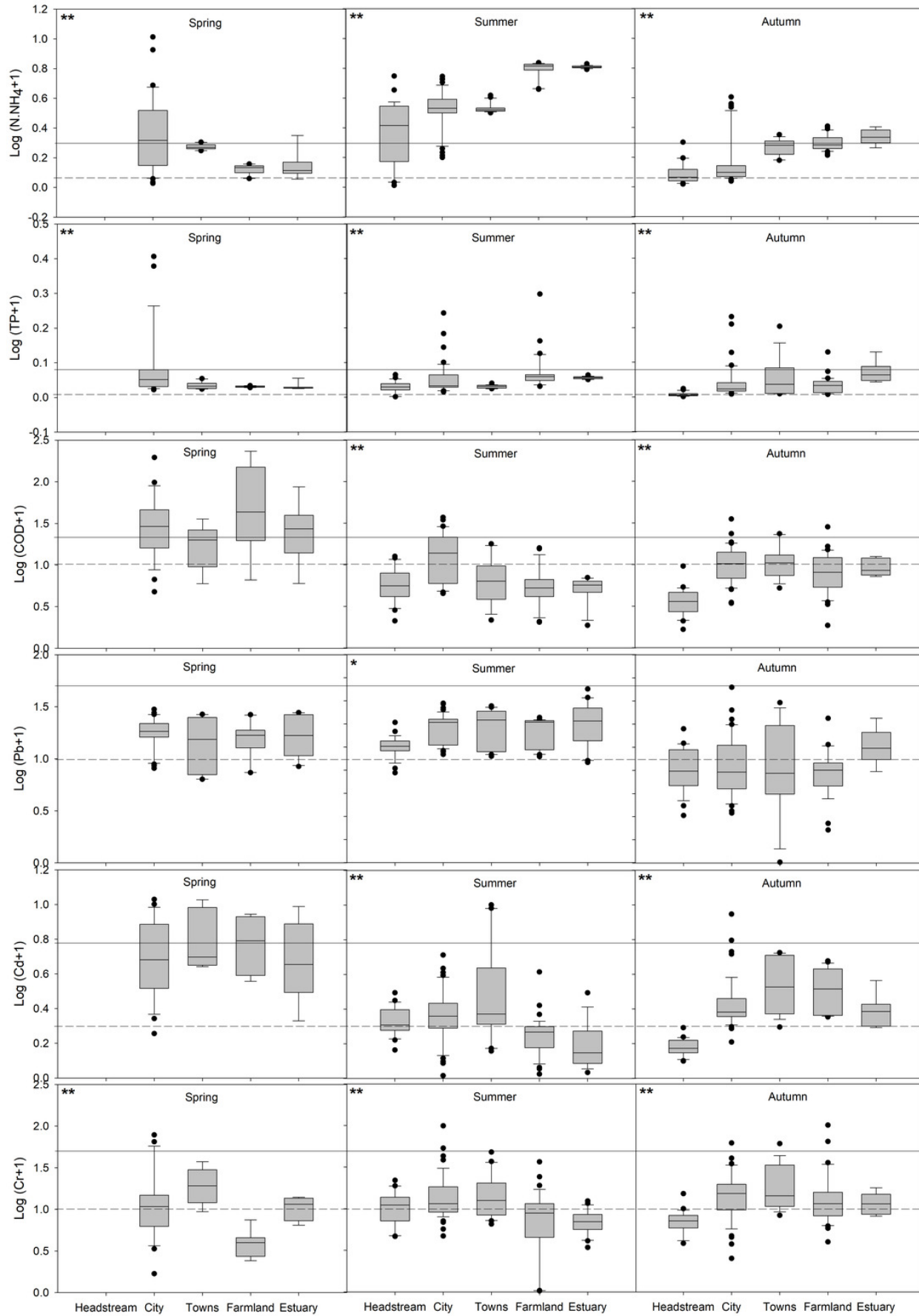


## Figure 4

Correlation matrix of eutrophic parameters and heavy metals in the water of FRS (A), and principal components of heavy metals in FRS (B)

In graph (A), the distribution of each variable was shown on the diagonal; the correlation values were shown in the upper triangular portion of the matrix; bivariate scatter plots with fitted lines were displayed in the lower triangular portion of the matrix; statistical significance levels were denoted as “\*\*\*”, “\*\*”, “\*” and “.” corresponding to p-values of <math><0.001</math>, <math><0.01</math>, <math><0.05</math> and <math><0.1</math>.

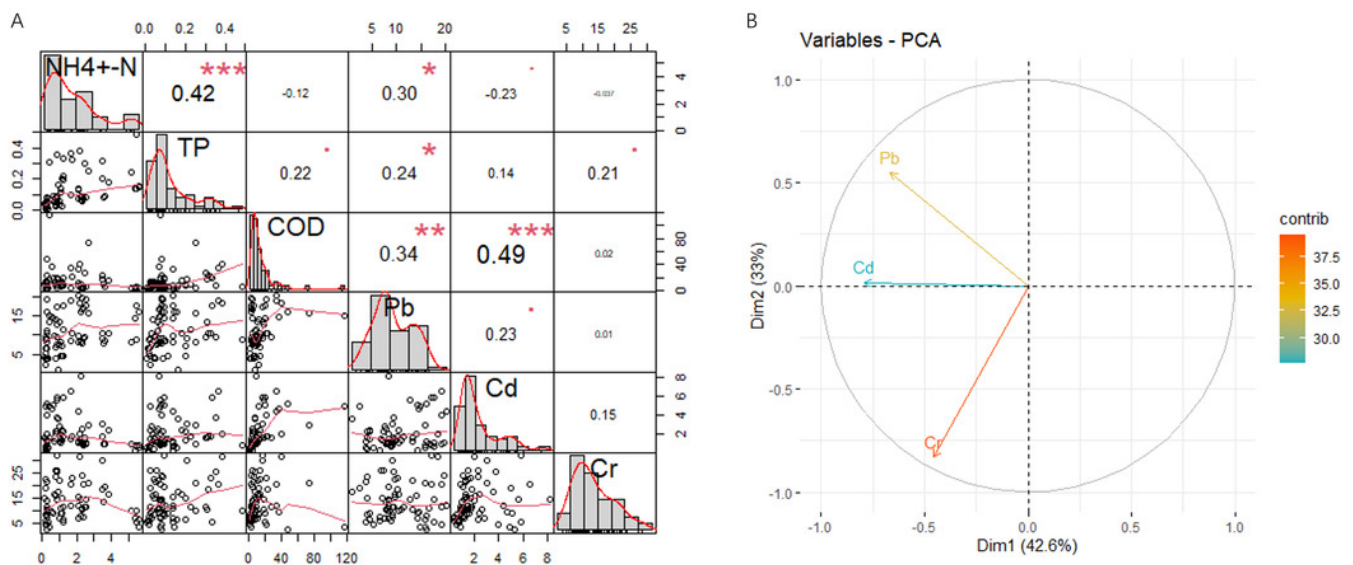


## Figure 5

Correlation between  $WQI$  of eutrophication ( $WQI_E$ , A) and heavy metals ( $WQI_{HM}$ , B) with the distance to the Baiyangdian estuary

$WQI_E$  and  $WQI_{HM}$  were calculated based on Class III and I of surface water standards, respectively. Filled points in the two graphs were measured in this study, and unfilled points in the graph (A) were measured by Environmental Protection Bureau of Baoding. Dash line was the correlation curve of summer  $WQI$  with the distance to the estuary and solid line was the correlation curve of autumn  $WQI$  in the two graphs, which were all statistical significance ( $p < 0.05$ ). Dotted line indicated the mean of all  $WQI$  values in each graph, and shaded area indicated the city area.

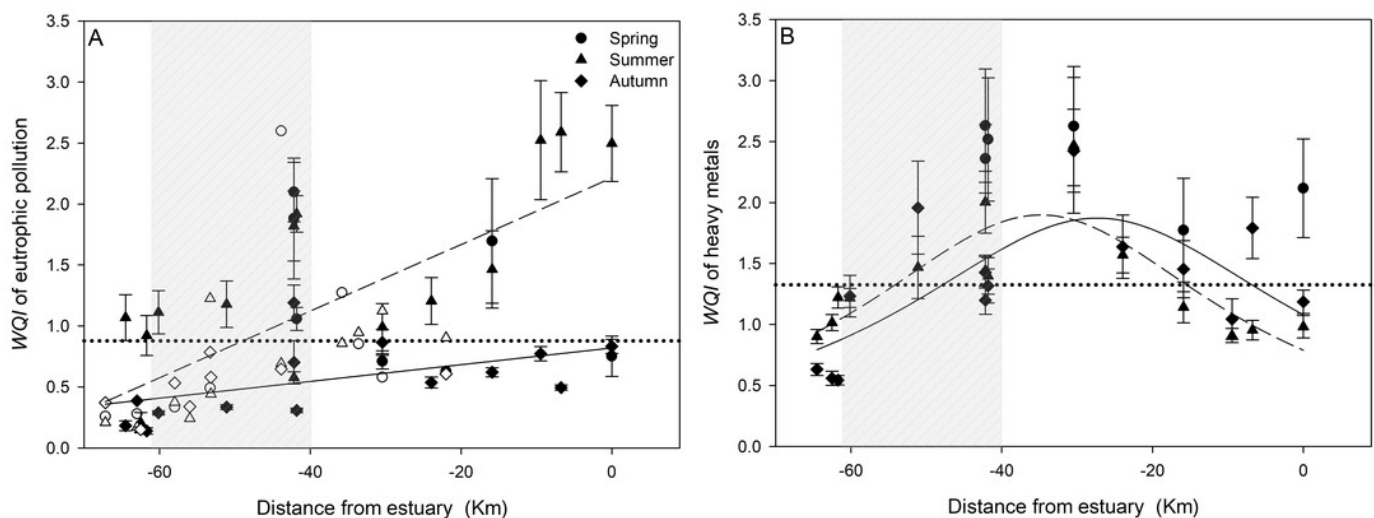


**Table 1** (on next page)

Changes of individual water pollution parameter when FRS flowed through the city area

North River: F2 and 8, Middle River: F3 and 7, South River: F1 and 6 in Fig. 1. SE = standard error of the mean. Superscript lowercase letter and capital letter of mean value indicated the differences among three rivers were statistical significance at the level  $p < 0.05$  and  $p < 0.01$ , respectively.

Summer		NH <sub>4</sub> <sup>+</sup> -N (mg·L <sup>-1</sup> )		TP (mg·L <sup>-1</sup> )		COD (mg·L <sup>-1</sup> )		Pb (μg·L <sup>-1</sup> )		Cd (μg·L <sup>-1</sup> )		Cr (μg·L <sup>-1</sup> )	
		mean	S.E.	mean	S.E.	mean	S.E.	mean	S.E.	mean	S.E.	mean	S.E.
<b>North river</b>	In	2.28	0.24	0.07 <sup>A</sup>	0.00	8.08 <sup>A</sup>	2.35	8.88	0.81	1.09 <sup>A</sup>	0.11	7.31 <sup>a</sup>	0.88
	Out	2.95	0.27	0.31 <sup>B</sup>	0.08	25.38 <sup>B</sup>	3.00	9.79	0.37	1.74 <sup>B</sup>	0.13	14.80 <sub>b</sub>	3.99
<b>Middle river</b>	In	1.89 <sup>A</sup>	0.23	0.12 <sup>A</sup>	0.01	5.93 <sup>A</sup>	1.21	9.01	0.46	1.40 <sup>A</sup>	0.19	13.67 <sup>A</sup>	1.23
	Out	3.68 <sup>B</sup>	0.24	0.19 <sup>B</sup>	0.01	16.40 <sup>B</sup>	2.25	9.84	0.91	2.71 <sup>B</sup>	0.31	23.13 <sub>B</sub>	5.48
<b>South river</b>	In	0.28 <sup>A</sup>	0.07	0.03 <sup>a</sup>	0.02	4.01 <sup>A</sup>	0.45	9.77	0.63	1.01	0.08	10.58 <sup>a</sup>	1.76
	Out	0.87 <sup>B</sup>	0.09	0.05 <sup>b</sup>	0.02	11.79 <sup>B</sup>	2.20	11.52	1.42	1.27	0.09	19.10 <sub>b</sub>	2.82
Autumn		NH <sub>4</sub> <sup>+</sup> -N (mg·L <sup>-1</sup> )		TP (mg·L <sup>-1</sup> )		COD (mg·L <sup>-1</sup> )		Pb (μg·L <sup>-1</sup> )		Cd (μg·L <sup>-1</sup> )		Cr (μg·L <sup>-1</sup> )	
		mean	S.E.	mean	S.E.	mean	S.E.	mean	S.E.	mean	S.E.	mean	S.E.
<b>North River</b>	In	0.29	0.11	0.01 <sup>A</sup>	0.00	4.01	0.69	6.64	1.41	0.67 <sup>A</sup>	0.05	5.65 <sup>A</sup>	0.54
	Out	0.27	0.04	0.07 <sup>B</sup>	0.01	6.17	0.84	9.78	1.83	1.72 <sup>B</sup>	0.29	12.12 <sub>B</sub>	1.67
<b>Middle River</b>	In	0.24 <sup>A</sup>	0.07	0.01 <sup>A</sup>	0.00	2.04 <sup>A</sup>	0.44	5.89	0.69	0.45 <sup>A</sup>	0.04	5.91 <sup>A</sup>	0.78
	Out	1.47 <sup>B</sup>	0.16	0.26 <sup>B</sup>	0.05	15.61 <sup>B</sup>	3.29	8.65	1.17	1.54 <sup>B</sup>	0.14	18.74 <sub>B</sub>	2.28
<b>South River</b>	In	0.20 <sup>a</sup>	0.04	0.03 <sup>A</sup>	0.01	2.44 <sup>A</sup>	0.30	5.26 <sup>A</sup>	1.07	0.43	0.05	7.18	1.09
	Out	0.33 <sup>b</sup>	0.03	0.20 <sup>B</sup>	0.08	15.91 <sup>B</sup>	2.88	10.84 <sub>B</sub>	1.50	1.56	0.15	9.40	1.75

1